Proc. Natl. Acad. Sci. USA
Vol. 90, pp. 3811–3814, May 1993
Biophysics

Atomic force microscopy of biochemically tagged DNA

MATTHEW N. MURRAY*†, HELEN G. HANSMA‡, MAGDALENA BEZANILLA‡, TAKESHI SANO§, D. FRANK OGLETREE¶, WILLIAM KOLBE*, CASSANDRA L. SMITH§, CHARLES R. CANTOR§, SYLVIA SPENGLER*, PAUL K. HANSMA‡, AND MIQUEL SALMERON¶

*Human Genome Center and ¶Material Science Division, Lawrence Berkeley Laboratory, Berkeley, CA 94720; ‡Department of Physics, University of California, Santa Barbara, CA 93106; and §Center for Advanced Biotechnology, Boston University, Boston, MA 02215

Contributed by Charles R. Cantor, December 24, 1992

ABSTRACT **Small fragments of DNA of known length were made with the polymerase chain reaction. These fragments had biotin molecules covalently attached at their ends. They were subsequently labeled with a chimeric protein fusion between streptavidin and two immunoglobulin G-binding domains of staphyloccocal protein A. This tetrameric species was expected to bind up to four DNA molecules via their attached biotin moieties. The DNA–protein complex was deposited on mica and imaged with an atomic force microscope. The images revealed the protein chimera at the expected location at the ends of the strands of DNA as well as the expected dimers, trimers, and tetramers of DNA bound to a single protein.**

The atomic force microscope (AFM) (1, 2) is a derivative of the better known scanning tunneling microscope (STM) (3). The AFM images by measuring and maintaining a constant load force exerted by a sharp probe as it scans over the surface. This characteristic of the AFM makes it ideally suited for imaging nonconducting samples like biological molecules. Several groups have previously used the AFM to image both single- and double-stranded DNA (4–13).

The demonstrated ability of the AFM to image DNA allows microscopists the opportunity to reembark on a series of experiments begun more than 30 years ago. Microscopists at that time tried to apply the newly developed ability of the transmission electron microscope (TEM) to image metal-shadowed DNA with the aim of mapping and sequencing this molecule. Attempts at sequencing DNA (14–16) with the TEM involved modifying DNA bases so that they would provide different, contrasting signals. Experiments designed to map DNA with the TEM involved both the imaging of sequence-specific proteins bound to the DNA (17) as well as the identification of probes hybridized to single-stranded DNA (18).

The AFM, due to its high resolution and its ability to image DNA under conditions where the native structure will be retained, offers the hope of being able to improve upon the mapping and sequencing work done by these early microscopists. To sequence DNA, the AFM must be able to differentiate between the four types of nucleotide base pairs. Present images of single-stranded DNA (9) do not offer sufficient resolution to observe the functional groups that distinguish one nucleotide base from another. However, other researchers have reported the ability to distinguish between pyrimidines and purines (nucleotide bases with one and two rings) in two-dimensional surface layers with the STM (19). These results suggest that, in the future, the resolution of the STM/AFM (scanning probe) instruments may be sufficient to determine the sequence of the nucleotides of DNA (20, 21).

In this paper we describe the imaging of DNA fragments marked at specific locations with protein tags. These results show that the AFM has sufficient resolution to map DNA. In its simplest form, mapping involves the measurement of the physical distance between two points along the DNA. In the experiments reported here, we have demonstrated the ability of the AFM to perform this task by attaching a large protein marker to genetically engineered pieces of human DNA and then measuring the known length from the protein marker to the other end of the DNA.

MATERIALS AND METHODS

DNA Preparation. The DNA used in the experiments was made by using the polymerase chain reaction to amplify a human DNA (*Alu*) sequence cloned into a pBR322 plasmid (22). Some of the commercially prepared primers (Operon Technologies, Alameda, CA) used had biotin (vitamin H) covalently attached to the first nucleotide in the primer. Two different lengths of DNA were made by using three different primers. The 353-base-pair DNA fragments had biotin at both ends, while the 701-base-pair DNA had biotin only at one end.

The protein used to mark the DNA was a chimera of streptavidin and two IgG-binding domains of staphyloccocal protein A (23). Streptavidin is a tetrameric protein that has an extremely high binding affinity ($K_B = 7.7 \times 10^{14}$ M^{-1} at pH 5) (24) for biotin. The addition of protein A served to increase the size of the streptavidin; it does not interfere with the ability of the streptavidin to bind four biotins (Fig. 1). The streptavidin was mixed with the biotinylated DNA at a molar ratio of approximately 2.5:1.

Preparation of Samples. Samples for microscopy were prepared on freshly cleaved ruby mica. Approximately 10 ng of the DNA solution in 1 μl of dilute TE buffer (10 mM Tris/1 mM EDTA, pH 8.0) was deposited on the mica and dried in vacuum. The images presented in this paper were taken after rinsing the sample with water while it was in the liquid cell of the microscope. It appeared that this rinse greatly aided in dissolving aggregates of DNA, which are seen before the rinse, into the individual monomers observed in the image.

Microscopy. The images presented here were obtained under 1-propanol with a Nanoscope II (Digital Instruments, Santa Barbara, CA) AFM. The cantilevers used were a NanoProbe prototype (Digital Instruments) and have an improved aspect ratio that led to the high lateral resolution obtained in these images.

Images were taken by recording the feedback signal used to maintain a constant force (height mode). The forces used were approximately 1 nanoNewton (nN), and the scan frequency was 7–9 Hz. The information density is 400 × 400 data points.

The publication costs of this article were defrayed in part by page charge payment. This article must therefore be hereby marked "*advertisement*" in accordance with 18 U.S.C. §1734 solely to indicate this fact.

Abbreviations: AFM, atomic force microscope; STM, scanning tunneling microscope.

†To whom reprint requests should be addressed.

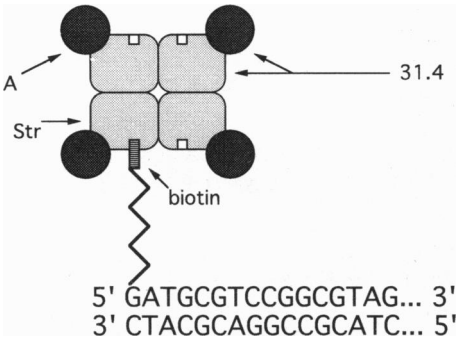

FIG. 1. Schematic of the chimeric protein fusion between tetrameric streptavidin (Str) and staphyloccocal protein A (A); 31.4 kDa indicates the mass of one of the four streptavin–protein A fusion subunits.

The length of the DNA was determined by measuring short straight stretches of the molecule with the image analysis software and then summing the values to determine the overall length. Protein and DNA dimensions presented in this paper were calculated by averaging 10 measurements taken from several representative images.

RESULTS AND DISCUSSION

We show in Fig. 2 a 1000 nm × 1000 nm image of the 353-base-pair DNA fragments on mica. The brighter spots at the ends of the strands represent higher points in the image, and are due to the protein complexes. The DNA appears firmly bound to the mica substrate; however, there is some indication of interaction between the tip and the chimeric protein tags on the lower right side of Fig. 2. The measured height at the protein site is almost twice that of the DNA, giving sufficient contrast for identification of the tag. The fragments appear in a variety of conformations, both as individual monomers as well as dimeric, trimeric, and tetrameric complexes bound at the ends.

By measuring individual DNA strands from the 353-base-pair preparation, we obtain a length of 105.8 nm with a standard deviation of 4.6 nm (Fig. 3 *Upper*).

Similar measurements on the 701-base-pair preparation gave a length of 196.9 nm (Fig. 3 *Lower*). In both cases the measured lengths are compatible with the expected values of 103.1 nm and 204.7 nm, respectively, for DNA in the A-form (25). The DNA was expected to convert to the dehydrated A conformation because the imaging was done in alcohol.

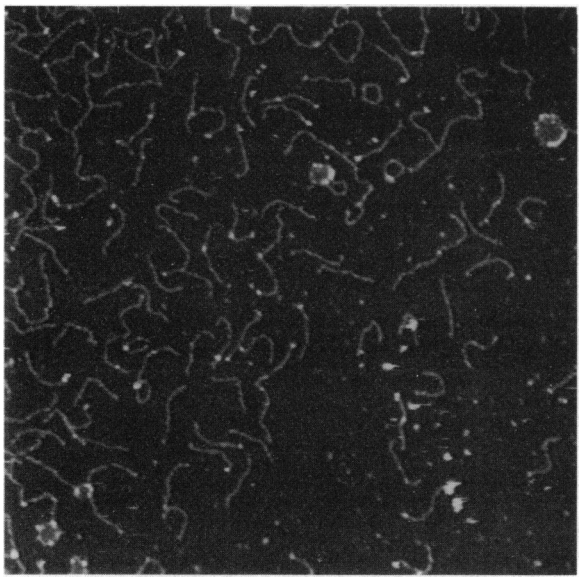

FIG. 2. A 1000 nm × 1000 nm image of 353-base-pair DNA. The length of the strands is 105.8 nm ± 4.6 nm. The average height of the protein tags (brighter spots) is 2.9 nm.

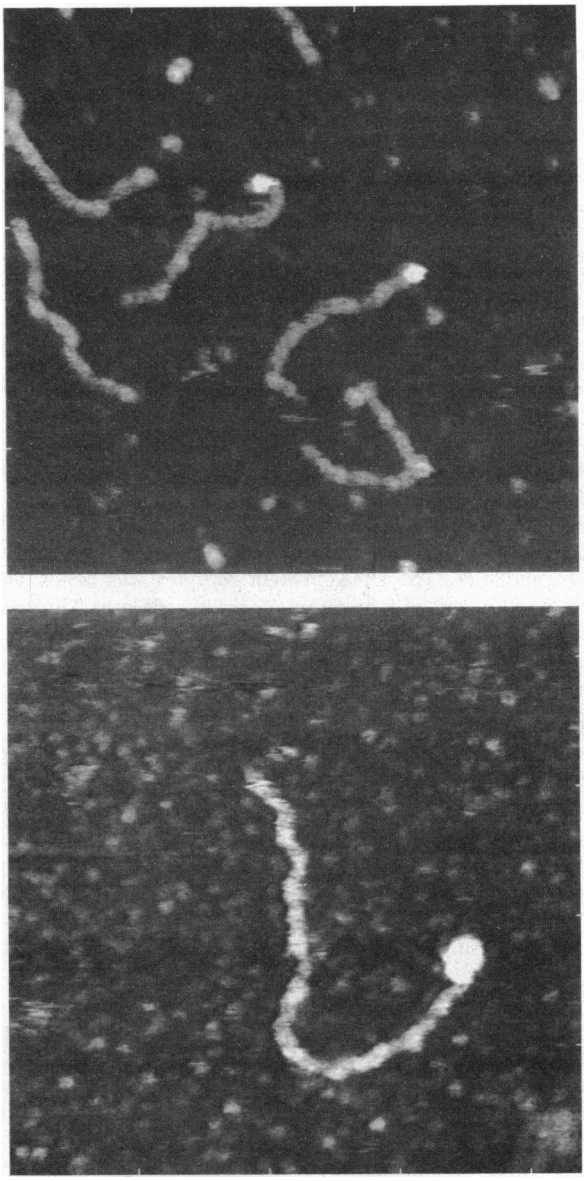

FIG. 3. (*Upper*) A 200 nm × 200 nm image of numerous strands of 353-base-pair fragments with and without their chimeric protein tags (brighter spots). (*Lower*) A 300 nm × 300 nm image of a 701-base-pair fragment labeled with its chimeric protein tag.

Many of the DNA strands are bound to the streptavidin–protein A chimeras, as can clearly be seen in the images. Fig. 4 shows a zoomed highlight of some of the aggregates. In Fig. 4 *Upper Left* we show DNA fragments that have circularized with biotins at each end of the strand attached to a single chimera molecule. Details of a dimer and trimer are shown in Fig. 4 *Upper Right* and *Lower Left*, respectively, while Fig. 4 *Lower Right* shows more examples of DNA aggregates, including a tetramer (near the center of the image). Extended matrices of 353-base-pair fragments could form, since they were biotinylated at both ends. No matrices were seen with the 701-base-pair DNAs that were biotinylated at only one end.

The measured width of the DNA was 7.8 nm, a value roughly 3 times larger than the DNA as revealed by x-ray diffraction (2.5 nm). The larger width in our AFM images is

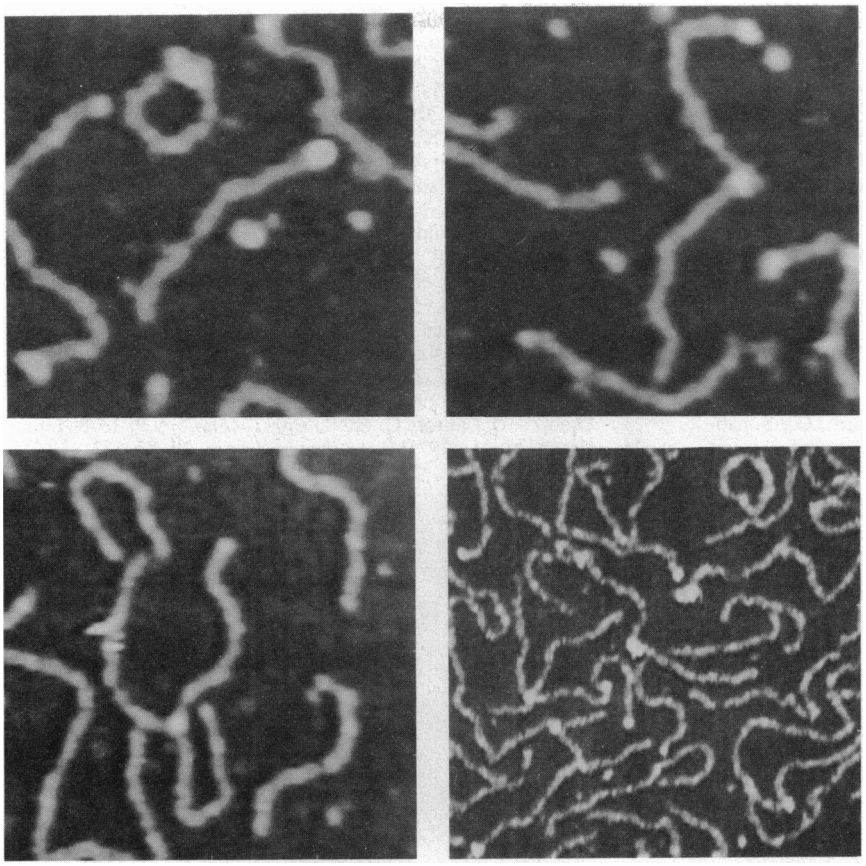

FIG. 4. These images have been extracted from larger area scans to emphasize certain forms of the DNA aggregates and are therefore at lower resolution. (*Upper Left*) A 180 nm × 180 nm image showing an example of a 353-base-pair fragment that has circularized with biotin molecules at each end bound to one chimera molecule. (*Upper Right*) A 195 nm × 195 nm image showing a dimer complex of two 353-base-pair fragments joined together by a chimera molecule. One of the DNA strands is labeled at the other end as well. (*Lower Left*) A 200 nm × 200 nm image showing a trimer with three 353-base-pair fragments joined by chimera molecule. The tip seems to have caught on one of the arms of the trimer during imaging. (*Lower Right*) A 325 nm × 325 nm image showing a tetramer (in the center left) as well as extended matrices of 353-base-pair DNA.

due to broadening by convolution with the finite tip shape (see Fig. 5).

The average height of DNA in our images (1.5 nm) was less than the expected value. This same effect has been reported by other researchers (4–13). There are several possible explanations for this discrepancy. The DNA itself probably suffers some elastic deformation because of the normal force exerted by the AFM tip (1 nN). Another contribution might be from a convolution of the cantilever deflection and rotation, which causes systematic errors in the measured signal. The average height of the protein complexes in our images was 2.9 nm.

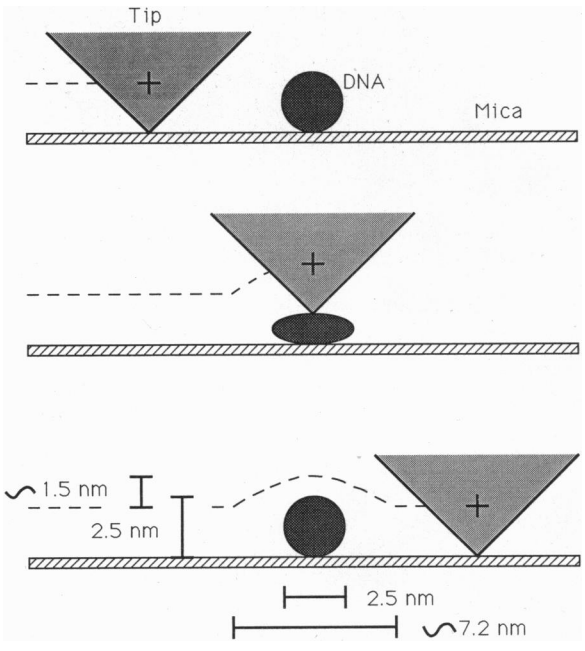

FIG. 5. Schematic of tip effects on the imaging of DNA. As the scanning tip moves from left to right, the first point of contact with the DNA is at the same height as the cross. Later, as the tip moves over the DNA fragment, the molecule may be compressed to some degree by the force exerted by the cantilever. The last point of contact between the tip and the DNA is on the left side of the tip at the same height as the cross.

While further improvements in tip sharpness and DNA orientation will be required for DNA sequencing, we have demonstrated sufficient resolution to identify markers on DNA. By attaching streptavidin complexes to selective sequences of DNA, the AFM should be able to map the location of these sequences on longer DNA molecules.

Note Added in Proof. This prediction has been supported by Shaiu *et al.* (4), who have recently taken images of plasmid DNA labeled with streptavidin-gold beads.

We gratefully acknowledge Mark Wendman for providing us with prototypes of the improved Nanotips and Prof. Sinsheimer for useful scientific discussions. This work has been supported by the Director, Office of Energy Research, Office of Basic Energy Sciences, Materials Science Division of the U.S. Department of Energy under Contract DE-AC03-76SF00098. Partial support has also been provided by National Science Foundation Grant DIR-9018846 (to H.G.H.), Digital Instruments, the Office of Naval Research, and the Creative Studies Department at the University of California, Santa Barbara (to M.B.).

1. Binnig, G., Quate, C. F. & Gerber, C. (1986) *Phys. Rev. Lett.* **56**, 930–933.
2. Rugar, D. & Hansma, P. (1990) *Phys. Today* **43** (10) 23–30.
3. Binnig, G., Rohrer, H., Gerber, C. & Weibel, E. (1982) *Phys. Rev. Lett.* **49**, 57–61.
4. Shaiu, W. L., Larson, D. D., Vesenka, J. & Henderson, E. (1993) *Nucleic Acids Res.*, in press.
5. Zenhausern, F., Adrian, M., ten Heggeler-Bordier, B., Emch, R., Taborelli, M. & Descouts, P. (1992) *J. Struct. Biol.* **108**, 69–73.

6. Bustamante, C. J., Vesenka, J., Tang, C. L., Rees, W., Guthold, M. & Keller, R. (1992) *Biochemistry* **31,** 22–26.
7. Vesenka, J., Guthold, M., Tang, C. L., Keller, D., Delaine, E. & Bustamante, C. (1992) *Ultramicroscopy* **42–44,** 1243–1249.
8. Hansma, H. G., Vesenka, J., Siegerist, C., Kelderman, G., Morrett, H., Sinsheimer, R. L., Bustamante, C., Elings, V. & Hansma, P. K. (1992) *Science* **256,** 1180–1184.
9. Hansma, H. G., Sinsheimer, R. L., Li, M. & Hansma, P. K. (1992) *Nucleic Acids Res.* **20,** 3585–3590.
10. Thundat, T., Warmack, R. J., Allison, D. P., Bottomley, L. A., Lourenco, A. J. & Ferrell, T. L. (1992) *J. Vacume Sci. Technol.*, in press.
11. Thundat, T., Allison, D. P., Warmack, R. J. & Ferrell, T. J. (1992) *Ultramicroscopy* **42–44,** 1101–1106.
12. Lindsay, S. M., Lyubchenko, Y. L., Gall, A. A., Shlyaktenko, L. S. & Harrington, R. E. (1992) *Proc. Soc. Photo-Opt. Intrum. Eng.* **1639,** 84–90.
13. Vesenka, J., Hansma, H., Siegrest, C., Siligardi, G., Schabtach, E. & Bustamante, C. (1992) *Proc. Soc. PhotoOpt. Intrum. Eng.* **1639,** 127–137.
14. Beer, M. & Moudrianakis, E. N. (1962) *Proc. Natl. Acad. Sci. USA* **48,** 409–416.
15. Moudrianakis, E. N. & Beer, M. (1965) *Proc. Natl. Acad. Sci. USA* **53,** 564–571.
16. Highton, P. J., Murr, B. L., Shafa, F. & Beer, M. (1968) *Biochemistry* **7,** 825–833.
17. Schleif, R. & Hirsh, J. (1980) *Methods Enzymol.* **65,** 885–896.
18. Wu, M. & Davidson, N. (1975) *Proc. Natl. Acad. Sci. USA* **72,** 4506–4510.
19. Allen, M. J., Balooch, M., Subbiah, S., Tench, R. J., Siekhaus, W. & Balhorn, R. (1991) *Scanning Microsc.* **5,** 625–631.
20. Hansma, H., Weisenhorn, A., Gould, S., Sinsheimer, R., Gaub, H., Stucky, G., Zaremba, C. & Hansma, P. (1991) *J. Vacume Sci. Technol.* **9,** 1282–1284.
21. Heckl, W. & Holzrichter, J. (1992) *Nonlinear* **1,** 53–59.
22. Deininger, P. L., Jolly, D. J., Rubin, C. M., Friedman, T. & Schmid, C. W. (1981) *J. Mol. Biol.* **151,** 17–33.
23. Sano, T. & Cantor, C. (1991) *Bio/Technology* **9,** 1378–1381.
24. Green, N. M. (1975) *Adv. Protein Chem.* **29,** 85–133.
25. Dickerson, R. E. (1983) *Sci. Am.* **252** (6) 94.